NUMERICAL MODELING OF DISCRETE SPATIAL HETEROGENEITY IN SEISMIC RISK ANALYSIS: APPLICATION TO TREATMENT OF LIQUEFIED SOIL FOUNDATIONS

F. Lopez-Caballero[(1)] , S. Montoya-Noguera [(2)]

[(1)] *Senior researcher, fernando.lopez-caballero@centralesupelec.fr*
[(2)] *PhD, smontoya@cityu.edu.hk, Present institution: Department of Architecture and Civil Engineering, City University of Hong Kong*
[(1,2)]*MSSMat CNRS UMR 8579 lab, CentraleSupélec, Paris-Saclay Univ., Châtenay-Malabry, France*

Abstract

A binary mixture model is proposed to study the effects on liquefaction-induced settlement after soil improvement based on the consideration of the added spatial variability between the natural and the treated soil. A 2D finite element model of a structure founded on a shallow foundation was coupled with a binary random field. Nonlinear soil behavior is used for both materials and the model is tested for different mesh size and input motions. Historical evidence as well as physical and numerical modeling indicates that improved sites present less liquefaction and ground deformation. In most cases this improvement is modeled as homogeneous however, in-situ measurements evidence the high level of heterogeneity in the deposit. Inherent spatial variability in the soil and the application -transportation, mixing, permeation - of some soil improvement techniques such as biogrouting and Bentonite permeations will necessary introduce heterogeneity in the soil deposit shown as clusters of the treated material in the natural soil.

Hence improvement zones are regarded as a two-phase mixture that will present a nonlinear relation due to the level of complexity of seismic liquefaction and the consequent settlement in a structure. This relation was shown to be in general independent to the sensibility with respect to the spatial discretization of the finite element model and the binary random field. However, it is greatly affected by the mechanical behavior of the soils used and the input motion. The effect on the latter can be efficiently related to the equivalent wave period.

Keywords: Seismic liquefaction; Soil improvement; Spatial variability

1. Introduction

Soil improvement techniques such as biogrouting and bentonite permeations, used to strengthen cohesive soils or to mitigate liquefaction are becoming widely used even though there remain some uncertainties given the spatial variability introduced in the design [1]. The success of these techniques is related to the effectiveness of the method - that is, how much of the soil is being changed - but also to its efficiency in improving the soil behavior - that is, how much are the consequences optimized. The effectiveness can be measured by the spatial fraction of the treated soil with respect to the total treatment area, for example the amount of gravel or clay introduced in a sand deposit. However, these techniques present an important uncertainty with respect to the final different spatial configurations on the vertical as well as in the horizontal direction. A success function relating effectiveness and the average efficiency could be defined in order to optimize the soil improvement consequences. To analyze the effects of added spatial variability due to soil improvement techniques a discrete auto-regressive code is coupled to a 2D finite element soil-structure interaction model. The former is used to generate the treated ground soil as a binary mixture composed of two materials: the reference soil and the added improved material. The latter is a two-story inelastic structure with a shallow foundation on loose-to-mediumsand (LMS). In the treatment zone, a medium-to-dense sand (MDS) is added. This work in part, contains material published in Montoya-Noguera and Lopez-Caballero [2].

This paper concerns the relation between the technique effectiveness and the average efficiency is evaluated for different input motions. To measure the latter, the relative surface settlement of the structure with respect to free field ($|u_z|$) at the end of shaking is used.

2. Numerical model

The numerical model used in this work corresponds to the reinforced concrete (RC) building with a shallow rigid foundation standing on saturated cohesionless soil presented in Montoya-Noguera and Lopez-Caballero [2]. A schema of the model is shown in Figure 1. The reference soil deposit is a 50m wide model composed of 20m of loose-to-medium sand (LMS) overlaying an elastic bedrock. The shear modulus increases with depth. The fundamental elastic period of the soil profile is equal to 0.38s. An elastoplastic multi-mechanism model is used to represent the soil behavior. Under the deposit, an engineering bedrock representing a half-space medium is modeled with an isotropic linear elastic behavior and a shear wave velocity (V_s) equal to 550m/s. The ground water table is located 1m below the surface. Concerning the treated ground soil the recommendations of Mitchell et al. [3] were used. By which height (H) should be given by the extension of the liquefiable layer, in this case H=4m below the water table, and length (L) should extend from the edge of the foundation of size B a distance bigger to the depth of treatment (i.e. $L > B + 2H$). The soil heterogeneity is simulated with a binary autoregressive model composed of two materials: a treated medium-to-dense sand (MDS) and the original loose-to-medium sand (LMS). A brief description of this model is given in section 2.5. For more information of the model refer to Montoya-Noguera and Lopez-Caballero [2].
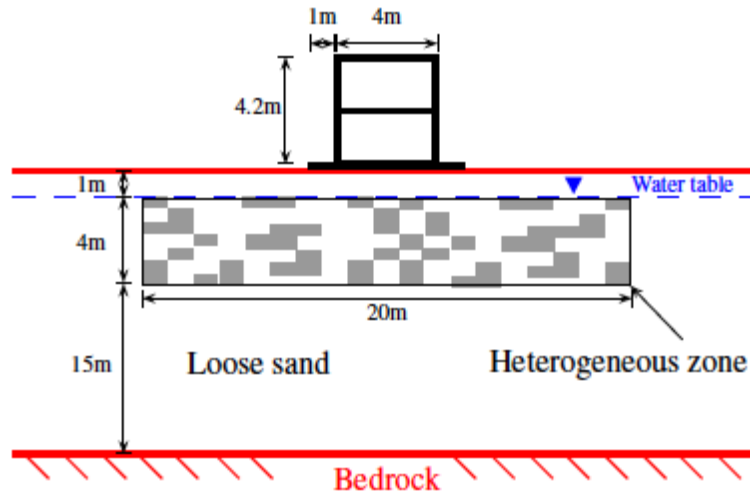
Fig. 1. Schema of the numerical model

2.1 Finite Element Model

As the soil is assumed to be horizontally homogeneous, a 2D finite element computation with plane-strain assumption was performed. It follows the simplified Biot's generalized consolidation theory [4] known as $\underline{u}$ - p_w formulation. The finite element code GEFDyn [5] was used. The saturated soil was modeled using quadrilateral isoparametric elements with eight nodes for both solid displacements and fluid pressures. The element size is 1m wide by 0.5m thick.

2.1.1 Boundary conditions

Concerning boundary conditions, as the signal propagation is 1D and the response of an infinite semi-space is modeled, equivalent boundaries have been imposed on the lateral nodes. For the bedrock's boundary condition, paraxial elements simulating "deformable unbounded elastic bedrock" have been used [6]. These elements efficiently evacuate diffracting waves in a local domain while the vertically incident shear waves, defined at the outcropping bedrock, are introduced into the base of the model after deconvolution. Thus, the obtained movement at the bedrock is composed of both incident and reflected waves. For the bedrock's boundary, the pore pressure conditions are assumed to be impervious. Therefore, no flux occurs across the interface boundary between the studied domain and the underlying semi-infinite space.

2.2 Structural model

For the sake of simplicity a two-story reinforced concrete (RC) building proposed by Vechio and Emara [7] is used. It consists of a large-scale one-span model with a shallow rigid foundation, standing on saturated cohesionless soil. The total structure height is 4.2m and the width is 4.0m. The mass of the building is equal to 45T and is uniformly distributed along beam elements, while the columns are supposed massless. The foundation is modeled as a rigid block of 0.1x6x4m. Between the structure's foundation and the soil, interface elements are used to allow relative movement of the structure with respect to the soil, in order to avoid the traction effect. These elements follow a Coulomb-type plastic criterion.

A scaled motion to a_{max}=1x10^{-5}g was used to evaluate the pseudo-elastic behavior of both soil and structure. The transfer function is the ratio between two acceleration wave fields and it gives information solely of the system between these two points. Figure 2 shows the transfer function (TF) of the free-field (surface/bedrock) and of the structure at fixed base and with soil-structure interaction (SSI) effects (top/FF). Regarding the structure, it can be seen that even if the building has two stories it behaves like a single-degree-of-freedom, as the second amplification peak is above 15Hz and of significantly less amplitude. The fundamental frequency (f_{str}), corresponding to the first peak, is equal to 4.16Hz.
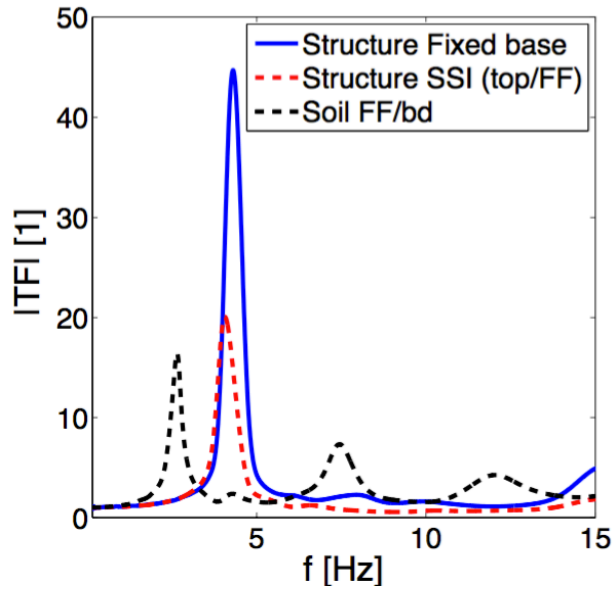
Fig. 2. Transfer function of the structure with fixed base and with SSI effect (top/FF) and of the soil deposit at free-field (surface/bedrock)

2.3 Binary random field model

The random field is generated with the homogeneous auto-logistic model derived by Bartlett and Besag [8]. It is a nearest-neighbor model defined as a conditional probability. That means it treats dependence directly through the so-called autocovariate, i.e. a function of the observations themselves. The binary mixture used to model the heterogeneous zone is defined with the spatial fraction $\gamma = N_1/(N_1 + N_2)$ where N_m is the number of elements of material m. From an engineering point of view, γ is related, for example, to the efficiency of a soil improvement technique, such as soil-mixing. Thus, could be calculated from the injected material with respect to the total area of intervention. Following the one-sided approximation, the expectation of x_{ij}, a value of the binary random variable X_{ij}, is given by:

$$E[x_{ij}|x_{i-1,j}, x_{i,j-1}] = \left[1 - \frac{1}{2}(\beta_1 + \beta_2)\right] \cdot \gamma + \frac{1}{2}(\beta_1 \cdot x_{i-1,j} + \beta_2 \cdot x_{i,j-1})$$

(1)

Where β1 and β2 are the auto-regressive coefficients that control the correlation length in the horizontal and vertical direction. Due to this approximation, the autocorrelation function ρ_{ij} is equal to $\beta^i_1\beta^j_2$, thus, it presents one step correlation in each direction. For each element, the generated probability is not a binary number, so it is compared to a random number (u_{ij}) that follows a uniform distribution function between 0 and 1, where each element is independent. This process, known as binarization, makes use of Monte Carlo simulations to converge to a given value. Further details on this model are presented in Montoya-Noguera and Lopez-Caballero [2].

2.4 Soil constitutive behavior

The elastoplastic multi-mechanism model used is the ECP model, developed at École Centrale Paris [9]. It uses a Coulomb type failure criterion and follows the critical-state concept. It can take into account a large range of deformations. For the cyclic behavior it uses a kinematic hardening, which relies on the state variables at the last load reversal. For a complete description of the model refer to Aubry et al. [9]; Hujeux [10]; and Lopez-Caballero [11] among others. The soil model parameters used in this study were determined with the procedure defined by Lopez-Caballero et al. [12] and can be found in Montoya-Noguera and Lopez-Caballero [2]. For this application the treated zone is composed of two materials: a treated medium-to-dense sand (MDS) and the

original loose-to-medium (LMS). The hydraulic conductivity (k_s) is also different for the two soils: 1×10^{-4}m/s for LMS and 1×10^{-5}m/s for MDS.

In order to analyze the differences concerning the liquefaction resistance, an undrained stress controlled cyclic shear test was simulated. The cyclic stress ratio ($SR = \tau/\sigma'_{v0}$) as a function of the number of loading cycles to produce liquefaction (N) is shown in Figure 3 for both soils. As a qualitative comparison, the modeled test results are compared with the curves given by El Mohtar et al. [13] for clean sand and sand with 3% of bentonite permeations. It is noted that the obtained curves are closer to the reference for clean sand corresponding to the LMS; while, the MDS curves are closer to those of a treated soil.
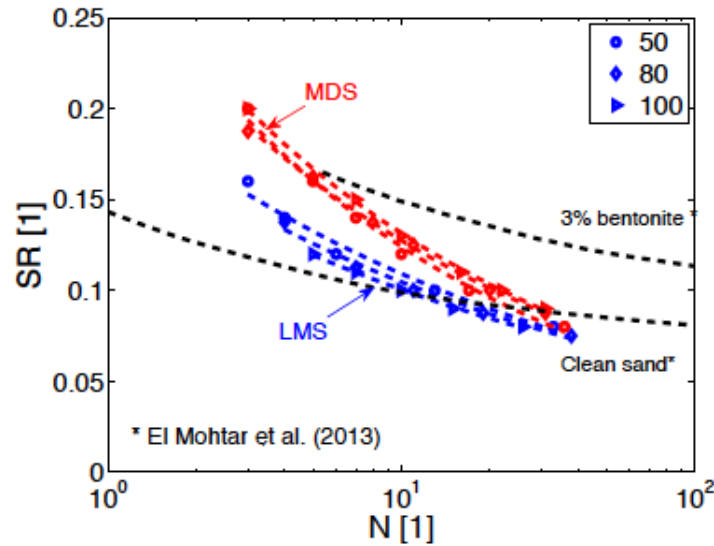

Fig. 3. Simulated liquefaction curves for both soils and comparison with results from El Mohtar et al. [13]

As an example, a zoom on the heterogeneous zone of two spatial distributions are shown in Figure 4 and correspond to a spatial fraction (γ) of 0.5 and auto-regressive coefficients (β_1 and β_2) equal to 0.4. As it can be seen, β does not give a constant correlation length in each row or column, but it is an average on the model. Similarly, γ is the average over the entire area; even though, there are regions with different composition as in the top left corner in Figure 4a.
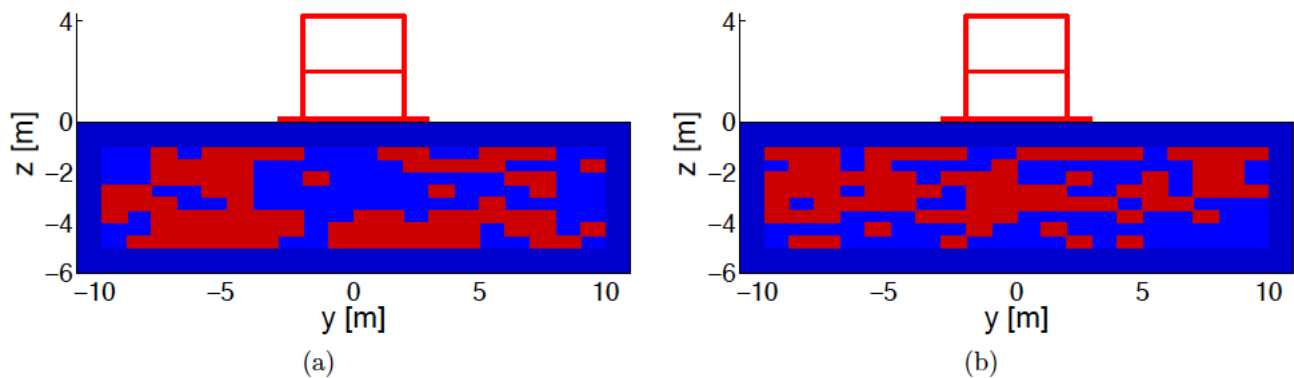

Fig. 4. Zoom on the heterogeneous zone for 2 distributions with $\gamma = 0.5$ and $\beta_1 = \beta_2 = 0.4$

2.5 Input earthquake motion

The computational cost of many random field simulations is important; hence a careful selection was performed to have strong input motions appropriate for the numerical model. Eight unscaled records were chosen from the Pacific Earthquake Engineering Research Center (PEER) database. The selected earthquake motions and some intensity measures (IM) are shown in Table 1. The IM shown are the peak horizontal acceleration (PHA), the Arias intensity (IA), the predominant duration (D_{5-95}) and the peak horizontal velocity (PHV). Figure 5 shows the normalized response spectra of the signals with a structural damping (ξ) of 5%. As the motions differ greatly in PHA, the results have been normalized in order to emphasize the differences in the frequency content.

Table 1: Input motions' identification and some intensity measures

#	Event	Year	RSN*	Mw	RJB	V_{s30}	PHA	IA	D_{5-95}	PHV
					[km]	[m/s]	[g]	[m/s]	[s]	[cm/s]
EQ1	Northridge 01	1994	1050	6.69	4.9	2016	0.43	1.79	9.84	51.23
EQ2	Kocaeli, Turkey	1999	1165	7.51	3.6	811	0.21	0.80	13.3	34.64
EQ3	Friuli, Italy02	1976	133	5.91	14.4	660	0.23	0.22	2.83	12.5
EQ4	Irpinia, Italy	1980	292	6.9	6.78	382	0.25	1.19	15.07	36.40
EQ5	LomaPrieta	1989	765	6.93	9.64	1428	0.41	1.05	6.53	31.57
EQ6	Northridge 01	1994	1012	6.69	9.87	706	0.25	0.93	8.07	27.39
EQ7	LomaPrieta	1989	810	6.93	18.41	714	0.40	2.04	9.66	17.53
EQ8	SanFernando	1971	77	6.61	1.81	2016.1	1.18	8.59	6.68	103.23

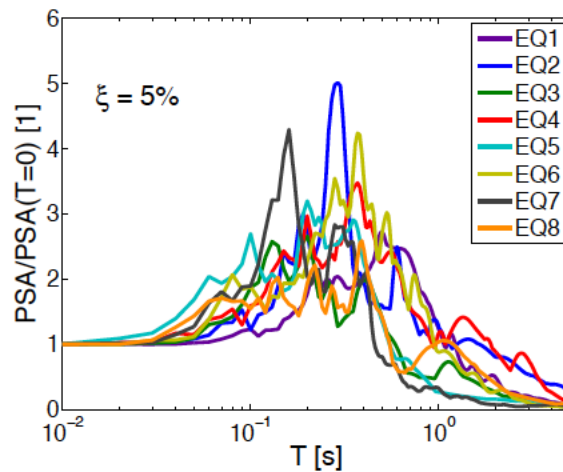*Record sequence number at the NGA database

Fig. 5. Normalized response spectra of acceleration.

3. Analysis and Results

The added spatial variability due to soil improvement is modeled with the binary random field described in section 1.3. The efficiency of the improvement technique is tested by varying the spatial fraction (γ) between not

treated to fully treated (i.e. from 1 to 0). 20 independent spatial distributions per value were realized. In this analysis, both auto-regressive coefficients (β_1 and β_2) are equal to 0.4 (i.e. a correlation length close to 8m). This value was taken from in-situ measurements and recommendations for sandy soil and gravelly sand [14, 15]. The effect in the liquefaction-induced settlement of different spatial correlations (e.g. magnitude of the correlation lengths and differences between the horizontal and the vertical correlations) could be interesting but it is out of the scope of this paper.

Figure 6 shows the box-and-whisker plots for the relative settlement of the structure with respect to free-field ($|u_z|$) as a function of the spatial fraction for two motions: EQ1 and EQ4. Dashed lines link the mean values, the boxes correspond to the 3 quartiles of data and the whiskers are the lowest and highest data within 1.5IQR (Inter-Quartile Range). Additionally, the results for two different mesh discretizations are shown.

Firstly, it can be seen that for both motions the mean settlement is reduced as more treated soil is added, i.e. as decreases. However, the rate or slope is not constant and differs for the two motions. For EQ1 for instance, it seems that even a small amount of treated soil (e.g. $\gamma = 0.9$) can reduce, in average, the relative settlement. In contrast, it appears that about $\gamma = 0.2-0.4$, the average settlement will not be greatly affected if a greater amount of treated soil is used. However, for EQ4 the curvature is different and the plateau is mostly seen for lower values. Regarding the variation for each value, i.e. with respect to the different spatial distributions, it can be observed that higher variation is present for γ equal to 0.5 and 0.4, respectively. This value could be the percolation threshold dividing the two curves, from which the interactions between the two soils change.
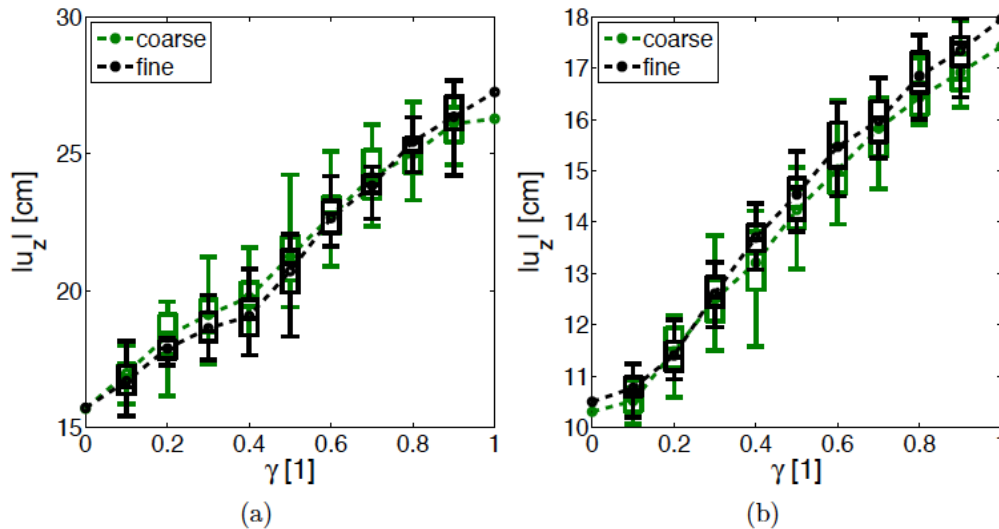

Fig. 6. Effect of the mesh size of the binary random field on $|u_z|$ for : a) EQ1 and b) EQ4

Concerning, the effect of the mesh discretization, it was analyzed by reducing the element size in the horizontal direction by half for the entire FEM. As expected, the average $|u_z|$ is slightly higher with the fine mesh for almost all values tested. However, the difference in the mesh discretization appears to affect all the spatial fractions similarly. In comparison the variation for each value is only slightly reduced with the fine mesh and is mostly noted for EQ4. Given that the results were not greatly changed, specially the relation with the different efficiencies, and that the numerical time of the fine mesh is significantly higher, the coarse mesh will be used for the rest of the analyses.

Figure 7a shows the mean $|u_z|$ as a function of γ for the eight motions tested. It is noted that the effect of the spatial variability is very different for each input motion but as the initial $|u_z|$ is also different, the relative difference defined as $\Delta|u_z| = (|u_z| - |u_{zMDS}|)/(|u_{z\,LMS}| - |u_{zMDS}|)$ is shown in Figure 7b. Note that the shape of the function, i.e. positive or negative concavity or s shape, appears to be related to other factors apart from the initial

|u_z| value. For instance, EQ2 and EQ7 have a similar |u_z| for the non-treated case however the former presents a positive concavity and the latter a negative one. This shape is related to the interactions between the two soils, though when the addition of a small fraction of treated soil affects only slightly the response and then for low γ values it drops, the relation has a positive concavity as for EQ2 and EQ5. In the other hand, when by only adding a small fraction, the settlement is drastically reduced while it is not greatly affected by a low γ value, the relation has a negative concavity as for EQ3 and EQ7. Concerning the other motions, a combination of both interactions is identified.
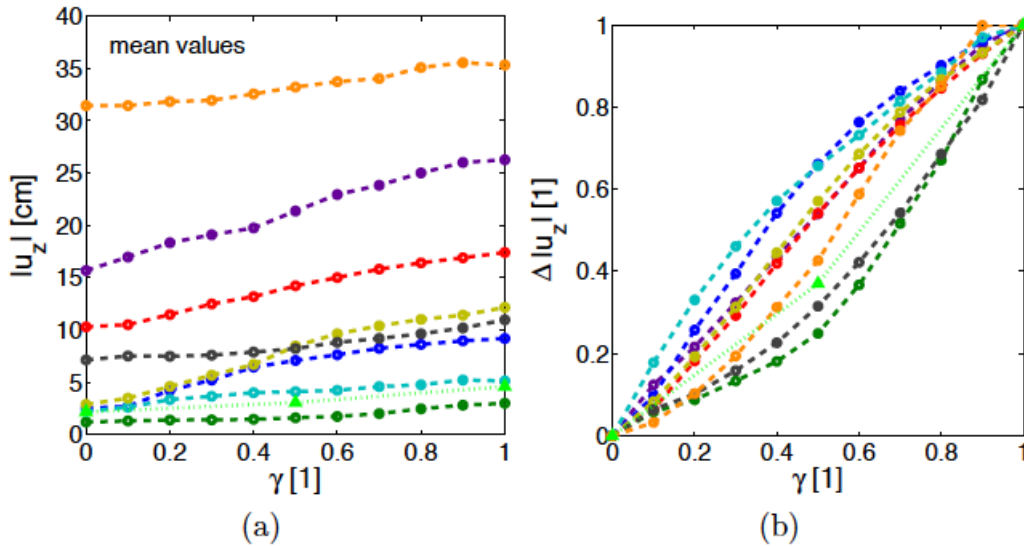

Fig. 7. |u_z| relation with γ for all motions tested: a) mean values and b) relative difference

In an effort to understand the relation between the input motion and the effect of the different spatial fractions, the value $\Delta|u_z|$ for $\gamma = 0.5$ was compared to 15 intensity measures (IM). Figure 8 shows the relation with the IM that presented the best relation: the period of equivalent harmonic wave ($T_{V/A}$). $T_{V/A}$ is the equivalent period corresponding to the intersection of the constant spectral acceleration and spectral velocity and is computed by:

$$T_{V/A} = 2\pi \frac{\alpha_V(\xi = 5\%)}{\alpha_A(\xi = 5\%)} \frac{PHV}{PHA} \text{ where } \frac{\alpha_V(\xi = 5\%)}{\alpha_A(\xi = 5\%)} = \frac{1.65}{2.12}$$

(2)

where α_V and α_A are the Newmark-Hall median spectrum amplification factors for the constant velocity and the constant acceleration regions with 5% damping. Green and Cameron [16] found a close relation between this IM and the amplification of soft soil sites. In this case, $T_{V/A}$ appears to better describe $\Delta|u_z|$ for $\gamma = 0.5$ as it takes into account the PHV as well as the inverse of the PHA. According to Kawase [17], $T_{V/A}$ is a simplified indicator of the dominant period of the motion, which appears to be related to the potential damage of structures. The PHV is commonly related to the shear strain demand of the motion and PHA, to its shear stress. In the same figure, the predominant period of the soil (T_0) and the structure (T^{FB}_{str}) is shown in solid and dashed lines, respectively. The differences of EQ3 and EQ5 with respect to the general trend can be due to the resonance with the soil for these motions.
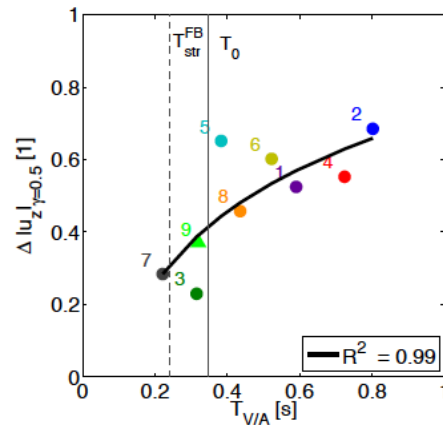
Fig. 8. Relation of the relative difference for γ=0.5 and $T_{V/A}$

4. Conclusions

A numerical model of discrete spatial heterogeneity was used to assess the liquefaction-induced settlement of an inelastic soil-structure system. The nearest-neighbor model introduced correlation in both directions. The effect of the spatial fraction (γ) of the treated-untreated soil mixture on the settlement was analyzed. At least twenty simulations were used for each γ. The main conclusions of the present study are:

- For all motions tested, the fully treated soil reduces the relative settlement of the structure with respect to free-field but the efficiency of the soil improvement varies for each input motion.

- With some motions, only a small amount of treated soil (i.e., high γ) can significantly reduce the relative settlement but then it is not greatly affected for low γ values; whereas, for other soils only when most of the soil is treated the relative settlement is reduced.

- The evolution of the relative settlement appears to be related to the period of equivalent harmonic wave ($T_{V/A}$) of the input motion. Hence the interaction between the two soils is affected by the ratio of the maximum acceleration and the maximum velocity.

5. Acknowledgements

6. References

[1] K. Kasama, A.J.Whittle, and K. Zen. (2012): Effect of spatial variability on the bearing capacity of cement-treated ground. *Soils and Foundations*, 52(4): 600–619.

[2] S. Montoya-Noguera and F. Lopez-Caballero (2016): Numerical modeling of discrete spatial heterogeneity in seismic risk analysis: Application to treated ground soil foundation. GeoRisk: Assessment and Management of Risk for Engineered Systems and Geohazards, 10(1): 66-82.

[3] J. Mitchell, H. Cooke and J. Schaeffer (1998): Design considerations in ground improvement for seismic risk mitigation. In *Geotechnical Earthquake Engineering and Soil Dynamics III*, Editors: Dakoulas, P., Yegian, M., and Holtz, R. D., volume 1, 580–613, Seattle, Washington. ASCE. Geotechnical Special Publication No. 75.

[4] O.C. Zienkiewicz and R.L. Taylor (1991): *The Finite element method, solid and fluid mechanics, dynamics and nonlinearity*, volume 2. McGraw-Hill Book Company, London, 4th edition.

[5] D. Aubry and A. Modaressi (1996): *GEFDyn - manuel scientifique*. Ecole Centrale Paris, France: MSSMat laboratory, July.

[6] H. Modaressi and I. Benzenati (1994): Paraxial approximation for poroelastic media. *Soil Dynamics and Earthquake Engineering*, 13(2): 117–129.

[7] F.J. Vechio and M.B. Emara (1992): Shear deformation in reinforced concrete frames. *ACI Structural journal*, 89(1): 46–56.

[8] M.S. Bartlett and J.E. Besag (1969): Correlation Properties of Some Nearest-Neighbor Models. *Bulletin of the International Statistical Institute*, 43(2): 191–193.

[9] D. Aubry, J.C. Hujeux, F. Lassoudiere, and Y. Meimon (1982): A double memory model with multiple mechanisms for cyclic soil behavior. In *International Symposium on Numerical Modeling in Geomechanics*, pages 3– 13, Balkema ed.

[10] J.C. Hujeux (1985): Une loi de comportement pour le chargement cyclique des sols. In *Génie Parasismique*, pages 278–302, France. Presses ENPC. Edited by V. Davidovici.

[11] F. Lopez-Caballero and A. Modaressi-Farahmand-Razavi (2010): Assessment of variability and uncertainties effects on the seimic response of a liquefiable soil profile. *Soil Dynamics and Earthquake Engineering*, 30(7): 600–613.

[12] F. Lopez-Caballero, A. Modaressi-Farahmand-Razavi and H. Modaressi (2007): Nonlinear numerical method for earthquake site response analysis i — elastoplastic cyclic model and parameter identification strategy. *Bulletin of Earthquake Engineering*, 5(3): 303–323.

[13] C. S. El Mohtar, A. Bobet, M. C. Santagata, V. P. Drnevich, and C. T. Johnston (2013): Liquefaction mitigation using bentonite suspensions. *Journal of Geotechnical Geoenvironmental Engineering*, 139(8): 1369–1380.

[14] E.E. Alonso and R.J. Krizek (1975): Stochastic formulation of soil properties. In *2nd Int. Conf. on Applications of Statistics and Probability in Soil and Structural Engineering*, volume 2, pages 9–32, Aachen.

[15] R. K. Senger, F. J. Lucia, C. Kerans, M. Ferris, and C. E. Fogg (1992): Geostatistical/Geological Permeability Characterization of Carbonate Ramp Deposits in Sand Andres Outcrop, Algerita Escarpment, New Mexico. In Permian Basin Oil and Gas Recovery Conference, pages 287–301, Midland, Texas.

[16] R.A. Green and W.I. Cameron (2003): The influence of ground motion characteristics on site response coefficients. In Pacific conference on earthquake engineering, page 19, University of Canterbury, Christchurch, New Zealand, February 2003. New Zealand Society for Earthquake Engineering. Paper No. 90 on CD.

[17] H. Kawase (2011): Strong ground motion characteristics and their damage impact to structures during the off pacific coast of tohoku earthquake of march 11, 2011; How extraordinary was this M9.0 earthquake? In 4th IASPEI / IAEE International Symposium: Effects of Surface Geology on Seismic Motion, page 13, University of California Santa Barbara.